

Debye–Waller parameter of palladium metal powders

M. INAGAKI, Y. SASAKI, M. SAKAI

Materials Science, Toyohashi University of Technology, Tempaku, Toyohashi 440, Japan

The Debye–Waller parameters were determined at room temperature and around 90 K for palladium metal powders with different particle sizes. The effective values obtained were divided into the dynamic component B_d , which is due to the thermal vibration of the constituent atoms and are temperature dependent, and the static component B_s , which is probably due to the static displacement of the atoms and is temperature independent. The Debye temperature θ_D calculated from the component B_d decreased with the increase in the component B_s , of which the relation was able to extrapolate to the θ_D -value determined on single crystals at $B_s = 0$. The decrease in θ_D was qualitatively explained by using a simple core-shell model, the shell part having as low a θ_D -value as 140 K.

1. Introduction

The temperature dependence of X-ray diffraction intensities has been interpreted by the thermal vibration of constituent atoms [1] and characterized by Debye–Waller parameter B . The diffraction intensity of the hkl line at a temperature, $I(hkl)$, is given as follows;

$$I(hkl) = k(LP)|F(hkl)|^2 pA \times \exp(-2B \sin^2\theta/\lambda^2) \quad (1)$$

where k is the so-called scale factor depending on the apparatus and its conditions employed, LP is the Lorentz–polarization factor, $|F(hkl)|^2$ is the structure amplitude, p is the multiplicity of the hkl line, A is the absorption factor, θ is the diffraction angle and λ is the wavelength of the X-rays used. The Debye–Waller parameter B is theoretically related to the Debye temperature θ_D ,

$$B = (6h^2T/mk\theta_D^2)[\phi(x) + (x/4)], \quad (2)$$

$$(x) = \frac{1}{x} \int_0^x \frac{\epsilon d\epsilon}{e^\epsilon - 1}, \quad x = \theta_D/T,$$

where h is Planck's constant, m is the mass, k is the Boltzmann constant and T is the ambient temperature. In monoatomic, isotropic crystals, it is

related to the mean square displacement $\langle u^2 \rangle$ of the atoms,

$$B = (8\pi^2/3)\langle u^2 \rangle. \quad (3)$$

The effective value of the Debye–Waller parameter B_{eff} can be experimentally determined as a slope of the line between the logarithmic values of the ratio of the observed intensities, $I_{\text{obs}}(hkl)$, to the theoretical intensities, $I_{\text{calc}}(hkl)$, and $\sin^2\theta/\lambda^2$ because Equation 1 is written as,

$$\ln [I_{\text{obs}}(hkl)/I_{\text{calc}}(hkl)] = \ln(k) - 2B_{\text{eff}} \sin^2\theta/\lambda^2 \quad (4)$$

where $I_{\text{calc}}(hkl) = (LP)|F(hkl)|^2 pA$.

The observed value of B_{eff} on a material was so different from sample to sample, that it seemed to depend on the physical state of the sample [2]. For example, it increased remarkably with grinding and decreased with annealing. One of the present authors and co-workers [3, 4] proposed to use the value B_{eff} as one of the characterization parameters of the powder materials, by showing its remarkable change with grinding and its experimental relations to the so-called lattice strain determined from the line broadening of X-ray diffraction on various materials. It has also been shown that the value of the Debye temperature calculated from the B_{eff} -value by Equation 2 is

TABLE I Experimental results

| Sample | Grain size (μm) | Ambient temperature (K) | B_{eff} (nm^2) | Debye \ddagger temperature (K) | B_{d} (nm^2) | θ_{D} (K) | B_{s} (nm^2) | Lattice strain | Crystallite size L (nm) |
|--------|---------------------------------|-------------------------------|---------------------------------------|--|-------------------------------------|----------------------------|-------------------------------------|----------------------|---------------------------------|
| A | 0.1 | 97 | 0.0108 | 100 | 0.0023 | 227 | 0.0085 | 4.1×10^{-3} | 14.4 |
| | | 297 | 0.0148 | 147 | 0.0063 | 227 | 0.0085 | | |
| B | ~ 0.1 | 115 | 0.0077 | 129 | 0.0028 | 220 | 0.0049 | 4.2×10^{-3} | 18.0 |
| | | 301 | 0.0117 | 167 | 0.0068 | 220 | 0.0049 | | |
| C | ~ 0.3 | 98 | 0.0082 | 116 | 0.0025 | 219 | 0.0057 | 4.5×10^{-3} | 19.6 |
| | | 299 | 0.0126 | 161 | 0.0069 | 219 | 0.0057 | | |
| D | ~ 0.7 | 95 | 0.0099 | 103 | 0.0024 | 221 | 0.0075 | 5.7×10^{-3} | 19.2 |
| | | 301 | 0.0142 | 152 | 0.0067 | 221 | 0.0075 | | |
| E | 0.2 \sim 0.7 | 98 | 0.0063 | 133 | 0.0024 | 226 | 0.0039 | 5.3×10^{-3} | 27.6 |
| | | 301 | 0.0104 | 178 | 0.0065 | 226 | 0.0039 | | |
| F | * | 86 | 0.0018 | 250 | 0.0017 | 262 | 0.0001 | 2.2×10^{-3} | 60.2 |
| | | 290 | 0.0048 | 258 | 0.0047 | 262 | 0.0001 | | |
| G | † | 86 | 0.0054 | 137 | 0.0021 | 231 | 0.0033 | — | — |
| | | 289 | 0.0093 | 184 | 0.0060 | 231 | 0.0033 | | |

* Annealed at 770 K for 1 h. See Fig. 1d.

† Mixture of samples B and F.

‡ Calculated directly from B_{eff} -value.

lower than that determined from the specific heat [5].

These experimental results suggests that the effective value of the Debye–Waller parameter determined by X-rays is larger than that expected from the specific heat, in other words, the mean square displacement detected by X-rays in Equation 3 contains an additional component in addition to the displacement due to the thermal vibrations of atoms. The component due to the thermal vibration can be called the dynamic component of displacement and this depends on time and temperature. The additional component, on the other hand, is supposed to be related to the static displacement of the atoms from their equilibrium positions in the crystal structure, which is probably associated with various defects, including the crystal surface. It is independent of time and temperature well below the annealing temperature of the defects.

If we calculate the mean square displacement $\langle u^2 \rangle$ by averaging over all atoms and time, which can be observed through X-ray diffraction, it is expressed by a simple sum of the mean square displacement of the dynamic and the static components, u_{d} and u_{s} ,

$$\langle u^2 \rangle = \langle u_{\text{d}}^2 \rangle + \langle u_{\text{s}}^2 \rangle. \quad (5)$$

Therefore, the effective Debye–Waller parameter B_{eff} observed must be composed of the dynamic

component B_{d} and the static component B_{s} ,

$$B_{\text{eff}} = (8\pi^2/3)[\langle u_{\text{d}}^2 \rangle + \langle u_{\text{s}}^2 \rangle] = B_{\text{d}} + B_{\text{s}}. \quad (6)$$

The presence of the static component B_{s} seems to make the B_{eff} -value larger than that expected from thermal vibration and also sensitive to the physical state of the sample.

In the present work, the values of B_{eff} were determined on different samples of the palladium metal powders and then divided into two components, B_{d} and B_{s} . We were able to successfully determine B_{d} and B_{s} on each sample, and a definite dependence of the Debye temperature θ_{D} on B_{s} was found. The extrapolation of θ_{D} to $B_{\text{s}} = 0$ gave the same value of θ_{D} as that reported on the single crystal.

2. Experimental details and results

Palladium metal powders were prepared by precipitation from palladium chloride in an aqueous solution with an organic reducing agent, such as hydrazine. Palladium metal was selected because of its monoatomic crystal, ease of preparation, simple face-centred cubic crystal structure, its stability in air and high atomic number. Seven samples with different grain sizes were prepared. The grain size determined from SEM (scanning electron microscopy) micrograph is tabulated in Table I and some of the SEM micrographs are shown in Fig. 1. The sample F was prepared by

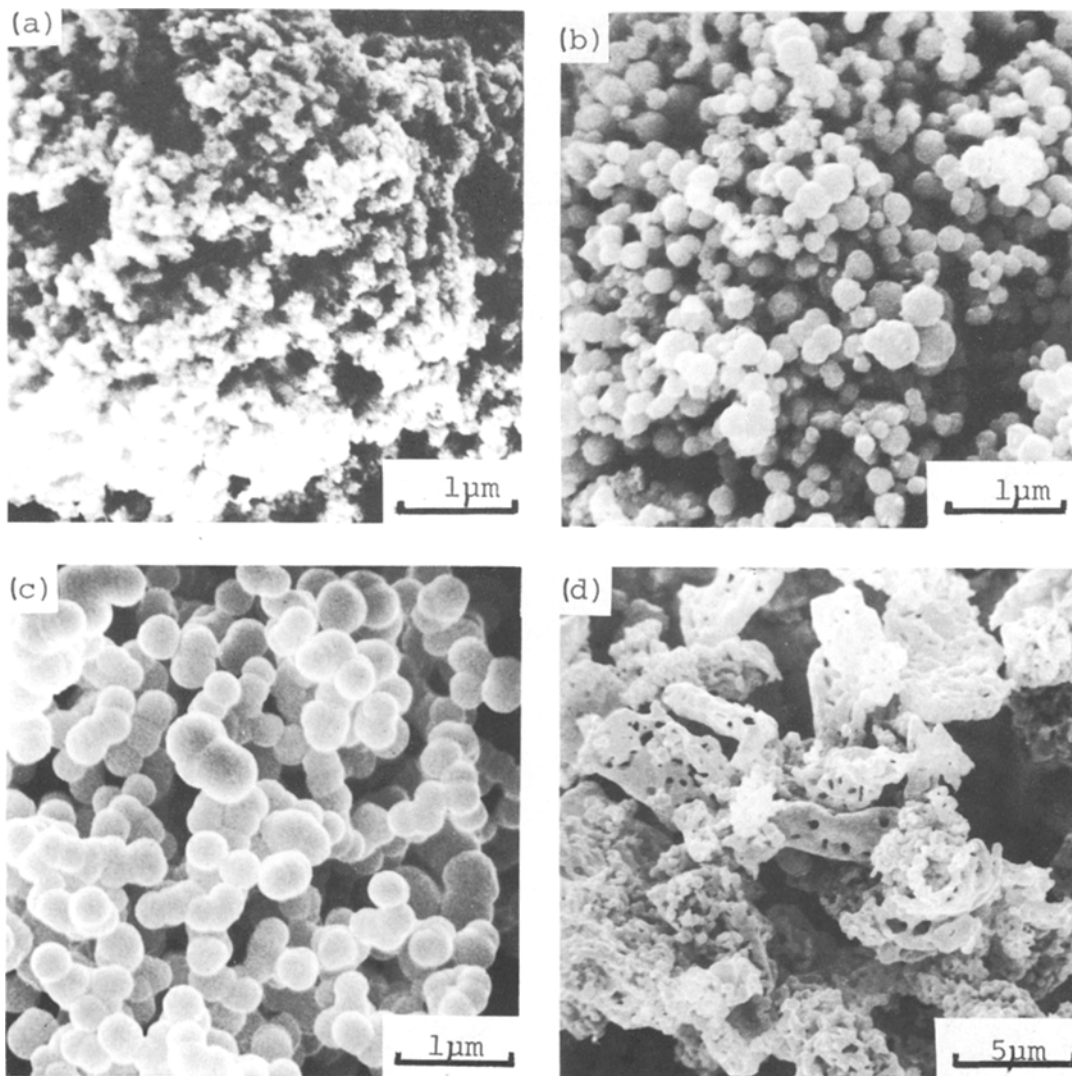


Figure 1 SEM micrographs of palladium metal powders used. (a) A, (b) D, (c) E and (d) F.

annealing sample A at 770 K for 1 h under a vacuum of 4×10^{-6} torr. The sample G was a mixture of samples B and F.

Eight diffraction lines were chosen in a wide range of $\sin^2\theta/\lambda^2$, each of which did not overlap with neighbouring lines. On each line, the integrated intensity $I_{\text{obs}}(hkl)$ was calculated by summing up the diffraction intensities measured in every 0.05° step in 2θ by the fixed time (40 sec) method and subtracting the background intensity. $\text{CuK}\alpha$ radiation filtered by nickel foil and a scintillation counter with a pulse height analyser were used. Diffraction intensity measurements were carried out at room temperature and at around 90 K.

The theoretical intensity for each line, $I_{\text{calc}}(hkl)$, was calculated from the structure

amplitude $|F(hkl)|^2$, the Lorentz-polarization factor, the multiplicity p and the absorption factor A evaluated from the bulk density of each powder sample. Because of the high bulk density ($\approx 1 \text{ g cm}^{-3}$), the high mass absorption coefficient ($206 \text{ cm}^2 \text{ g}^{-1}$) and the thick specimen (1 mm), the absorption factor was constant over the range of $\sin^2\theta/\lambda^2$ used.

Linear relations between $\ln [I_{\text{obs}}(hkl)/I_{\text{calc}}(hkl)]$ and $\sin^2\theta/\lambda^2$ were observed on all samples, as shown in Fig. 2. The B_{eff} -values determined from the slope of these lines are summarized in Table I. The accuracy in the B_{eff} -value seemed to be about $\pm 0.0002 \text{ nm}^2$ and that in θ_{D} -value calculated from B_{eff} -value was about 6° .

On each sample, the lattice strain ϵ and

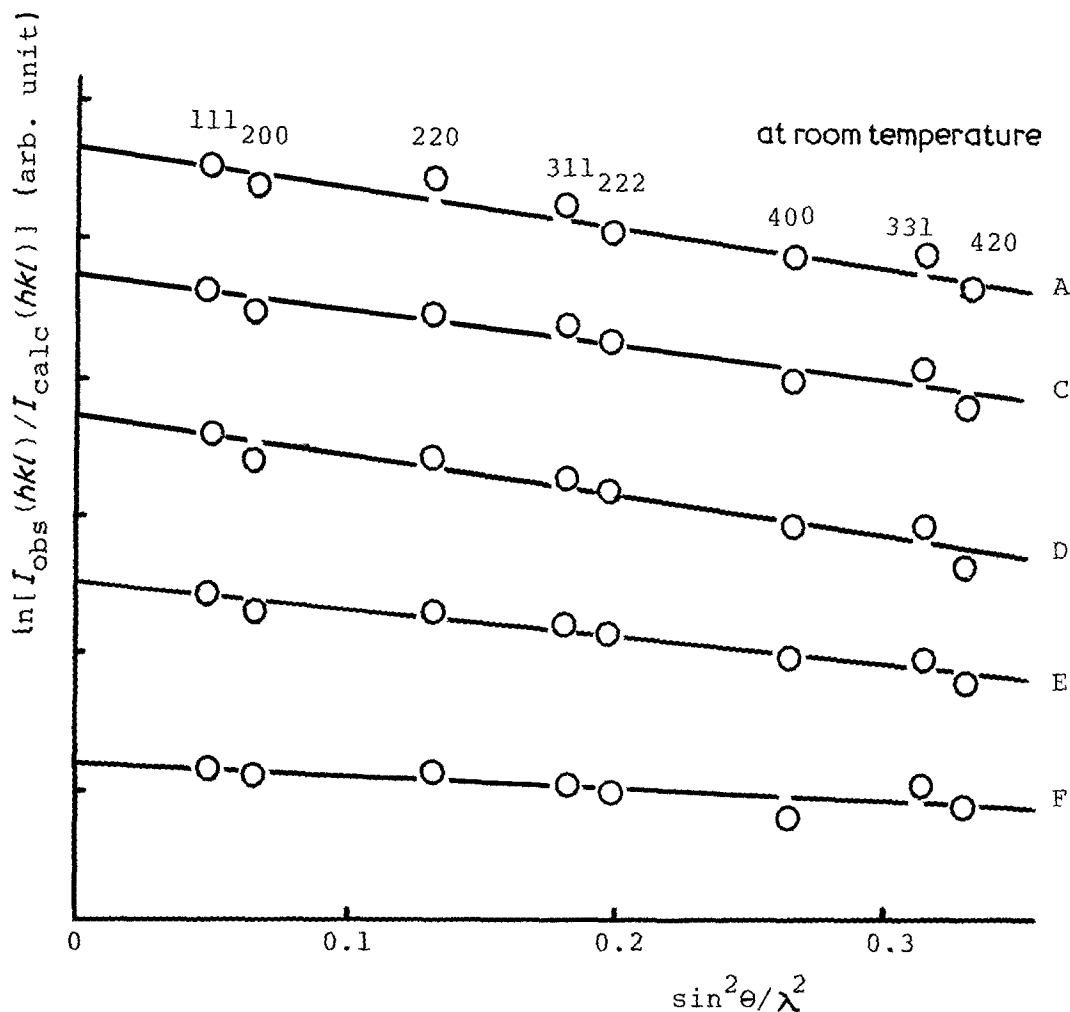


Figure 2 Plots of $\ln [I_{\text{obs}}(hkl)/I_{\text{calc}}(hkl)]$ against $\sin^2 \theta/\lambda^2$.

crystallite size L were determined from half-widths β of the diffraction profiles of the lines according to the following relation [6],

$$\beta \cos \theta/\lambda = 0.89/L + 2\epsilon \sin \theta/\lambda. \quad (7)$$

The results are also shown in Table I.

3. Discussion

3.1. Determination of the components B_d and B_s

The B_{eff} -values spread over a wide range; at room temperature, for example, from 0.0048 for the annealed sample F to 0.0148 for sample A with the smallest grain size. The grain size determined under SEM (Table I) is the apparent size of secondary particles, aggregates of small crystals as shown by the crystallite size determined from X-ray line broadening. Samples D and E have similar size, the latter containing the grains with

the smaller size, but the B_{eff} -values for these samples are quite different. The latter shows smaller B_{eff} -value and a much larger crystallite size L . The Debye temperatures calculated directly from the B_{eff} -value, by neglecting the static component B_s , are different at two ambient temperatures. On the annealed sample F, the differences in these θ_D -values is 8° , which is within the experimental accuracy for θ_D . For the other samples, however, the differences are 40 to about 50° , largely beyond the accuracy. All of the θ_D -values observed in the present work are much smaller than the value 276 K reported on the single crystal [7]. These results strongly support the presence of the static component B_s in addition to the dynamic component B_d in B_{eff} .

Because the static component B_s in B_{eff} is assumed to be independent from temperature, the difference between B_{eff} -values $B_{\text{eff}}(T_a)$ and

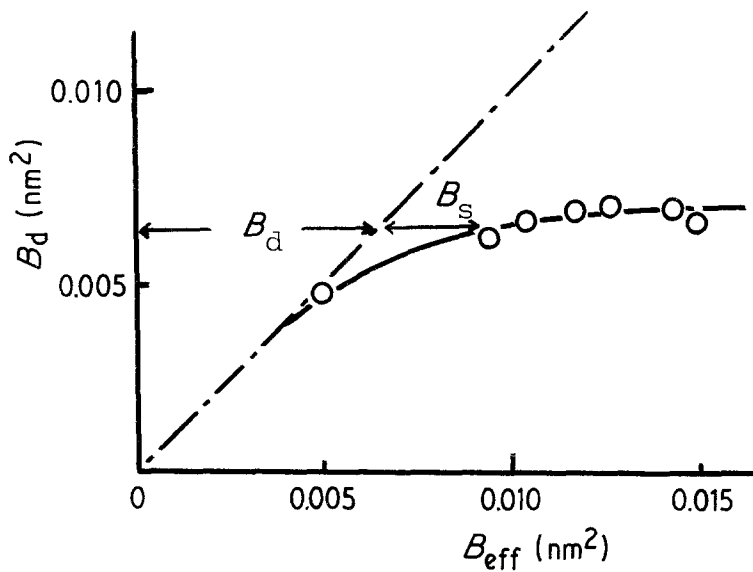


Figure 3 Relation between effective value of Debye-Waller parameter B_{eff} and the dynamic component B_{d} on palladium metal powders.

$B_{\text{eff}}(T_{\text{b}})$ measured at two different temperatures T_{a} and T_{b} equals the difference in the dynamic component B_{d} which follows Equation 2. By taking account of $T_{\text{a}}/T_{\text{b}} = n$ and from Equations 2 and 6, the following equations can be written

$$\begin{aligned} B_{\text{eff}}(T_{\text{a}}) - B_{\text{eff}}(T_{\text{b}}) &= B_{\text{d}}(T_{\text{a}}) - B_{\text{d}}(T_{\text{b}}) \\ &= (6h^2/T_{\text{a}}mk)\{f(x_{\text{a}}) - nf(nx_{\text{a}})\}, (8) \\ f(x) &= \frac{1}{x} [\phi(x) + x/4], \quad x = \theta_{\text{D}}/T. \end{aligned}$$

By using the measured difference of $B_{\text{eff}}(T_{\text{a}}) - B_{\text{eff}}(T_{\text{b}})$, therefore, we can solve Equation 8 numerically and determine the x_{a} -value, that is, the Debye temperature θ_{D} . From θ_{D} thus determined, B_{d} -values at different temperatures and then B_{s} -values can be determined.

In Fig. 3, the dynamic component B_{d} at room temperature, thus determined, is plotted against B_{eff} . The deviation of the B_{eff} -value from the line $B_{\text{eff}} = B_{\text{d}}$ (that is, $B_{\text{s}} = 0$) corresponds to the value of B_{s} . The present relation shows that the increase in B_{eff} is largely due to the increase in the B_{d} component. Up to 0.013 nm^2 for B_{eff} , the B_{s} component is less than the B_{d} component, but above 0.013 nm^2 the B_{d} component remains almost constant and the increment in B_{eff} is largely due to the increase in B_{s} .

3.2. Debye temperature of powders

The value of the Debye temperature determined from Equation 8 is less than that reported on the single crystal, 276 K [7], the annealed sample F having the nearest value (Table I). It is widely

known that the surface layer has a much smaller value of θ_{D} than the bulk. With palladium metal, the surface Debye temperature was determined as 140 K by LEED (low energy electron diffraction) [8]. In the present work, the smaller crystallite size tends to correspond to a lower value of θ_{D} . The smallest θ_{D} -value observed, however, is 220 K because the θ_{D} -value determined here is the value averaged over all the atoms, either at the surface or the inside of the crystallites.

If we assume a simple model of spherical crystallites which consists of two parts, a core and a surrounding shell, and characteristic Debye temperature for each part, θ_{core} and θ_{shell} , the observed dynamic component B_{d} is expressed by the sum of the dynamic components for the core B_{dc} and that of the shell B_{ds} as follows,

$$B_{\text{d}} = \alpha B_{\text{ds}} + (1 - \alpha) B_{\text{dc}}. \quad (9)$$

If the atomic fraction in the shell α is approximated by the volume fraction of the shell,

$$B_{\text{d}} = B_{\text{dc}} + \frac{3\Delta r}{r} (B_{\text{ds}} - B_{\text{dc}}), \quad (10)$$

where r is the radius of the spherical crystallites and Δr the thickness of the shell. This relation B_{d} against $1/r$ gives the value of B_{dc} by extrapolation to $1/r = 0$, which gives θ_{core} from Equation 2. Either Δr or θ_{shell} through B_{ds} can be evaluated from the slope of this relation by knowing θ_{shell} or Δr , respectively.

The linear relationship between B_{d} and $1/r$ is confirmed on the present sample by using half of the crystallite size as r , as shown in Fig. 4. The

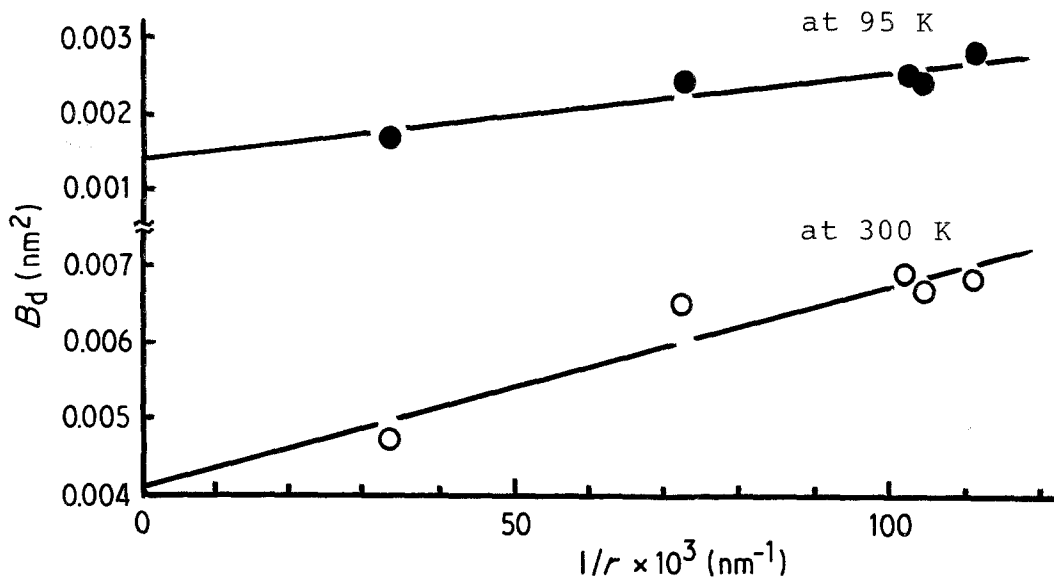


Figure 4 Dependence of the dynamic component B_d on the inverse of crystallite radius $1/r$ at 95 and 300 K.

dynamic component for the core, B_{dc} , obtained by the extrapolation gives the Debye temperature of about 280 K, which coincides with that for the single crystal. On the surface of the palladium metal, the Debye temperature of 140 K has been reported [8]. By assuming the value calculated from 140 K as B_{ds} , the thickness of the shell part Δr was determined as about 0.8 nm. This thickness roughly corresponds to that of 3 to 4 atomic layers. The fraction α of the shell is about 27% for the sample B with the average radius of 9.0 nm, for example.

The atoms on the surface layer of crystallites are reasonably supposed to have larger static displacement, which causes the increase in the value

of B_s . In Fig. 5, θ_D is plotted against B_s . The value of θ_D is found to be closely related to the value of B_s . This relation can be extrapolated to the value of 276 K at $B_s = 0$, which coincides with the value reported on the single crystal. A similar relation was obtained on another material, PbS powders [9].

The core-shell model employed here is evidently oversimplified; perfectly spherical crystallites, clear boundary between core and shell parts, etc. not being expected in practice. However, the present discussion strongly suggests the importance of the static component B_s in B_{eff} and the remarkable lowering of the Debye temperature at the surface layer of the crystallites. Harada *et al.* [10]

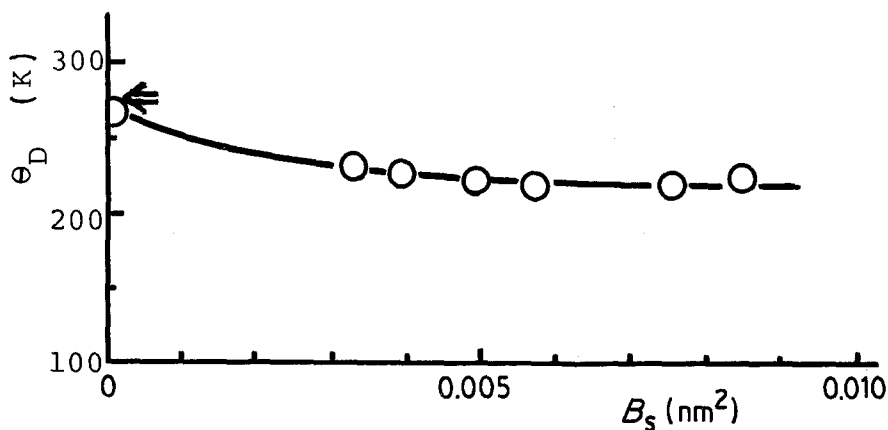


Figure 5 Relation between the static component B_s and the Debye temperature θ_D on palladium metal powders. The arrow shows the Debye temperature on the single crystal [7].

measured the low value of Debye temperature on fine gold powders, the lower values being for the smaller particle size, and explained the result by using a core-shell model.

3.3. Mean square displacement of atoms and melting

For palladium, the Debye temperature of 276 K and the melting point of 1823 K have been reported. By combining Equations 2 and 3, the mean square displacement of the atoms at the melting point was calculated at about 0.001 nm^2 . This corresponds to about 0.032 nm of the root mean square amplitude of vibration, being about 12% of the interatomic distance. This means that we recognize the melting of palladium when the mean square displacement is over 0.001 nm^2 , in other words, when the r.m.s. amplitude of vibration exceeds 12% of interatomic distance.

The surface layer of the palladium metal which has a much lower θ_D , as low as 140 K, gives the mean square displacement $\langle u_a^2 \rangle$ of 0.001 nm^2 at 470 K, that is, it seems to have as low a melting point as 470 K. On the sample F, which was prepared from sample A by annealing at 770 K for 1 h, the coagulation of the grains was observed, as shown in Fig. 1. This indicates a local melting of the palladium metal at the surface layer of the particles. This observation agrees qualitatively with the above discussion; the surface layer, shell part, has a lower Debye temperature and a lower melting point.

The mean square displacement due to thermal vibration at 300 K, which is calculated from

B_a by Equation 3, is about 0.00023 to about 0.00026 nm^2 , except 0.00018 for the annealed sample F. These values correspond to the r.m.s. amplitude of vibration of 0.015 to about 0.016 nm , about 5% of the interatomic distance. The mean square displacement $\langle u_g^2 \rangle$ calculated from the static component B_s is from 0.00 for the annealed sample F to 0.0003 nm^2 for sample A. The influence of this static displacement on the melting phenomena needs to be studied in further detail.

References

1. P. DEBYE, *Ann. Phys.* **43** (1914) 29.
2. M. INAGAKI, H. FURUHASHI, T. OZEKI, H. MUGISHIMA and S. NAKA, *J. Mater. Sci.* **6** (1971) 1520.
3. M. INAGAKI, H. FURUHASHI, T. OZEKI and S. NAKA, *ibid.* **8** (1973) 312.
4. M. INAGAKI and S. NAKA, *Zairyo* **27** (1978) 604.
5. N. SINGH and P. K. SHARMA, *Phys. Rev. B* **3** (1971) 1141.
6. H. P. KLUG and L. E. ALEXANDER, "X-ray Diffraction Procedures" 2nd edn. (Academic Press, New York, 1974).
7. N. T. PADIAL, L. M. BRESCANSIN and M. M. SHUKLA, *Acta Phys. Pol. A* **57** (1980) 129.
8. J. M. MORABITO, R. F. STEIGER and G. A. SOMOYAI, *Phys. Rev.* **179** (1969) 638.
9. M. INAGAKI, Y. SASAKI and M. SAKAI, to be published.
10. J. HARADA, S. YAO and A. ICHIMIYA, *Acta Cryst.* **A31** (1975) 204.

*Received 21 September
and accepted 23 November 1982*